Investigation of light trapping effect in hyperbolic metamaterial slow-light waveguides

2015 Appl. Phys. Express 8 082601

(http://iopscience.iop.org/1882-0786/8/8/082601)

Applied Physics Express **8**, 082601 (2015)
http://dx.doi.org/**10.7567/APEX.8.082601**

Investigation of light trapping effect in hyperbolic metamaterial slow-light waveguides

Borui Li[1], Yingran He[1,2], and Sailing He[1,3*]

[1]*Centre for Optical and Electromagnetic Research, Zhejiang Provincial Key Laboratory for Sensing Technologies, Zhejiang University, Hangzhou 310058, China*
[2]*The 54th Research Institute of CETC, Shijiazhuang 050081, China*
[3]*Department of Electromagnetic Engineering, JORCEP, School of Electrical Engineering, Royal Institute of Technology (KTH), S-100 44 Stockholm, Sweden*
E-mail: sailing@kth.se

Received May 26, 2015; accepted June 26, 2015; published online July 13, 2015

A hyperbolic metamaterial waveguide can reduce the group velocity of light down to zero by tuning a waveguide structure. The light trapping capability of a tapered hyperbolic metamaterial waveguide is comprehensively studied in this work. Although a pulse of light cannot be trapped forever in such a waveguide, the duration that light remains trapped can be flexibly prolonged by adjusting the volume filling ratio of the metamaterial or the material dispersion, in order to achieve a sufficiently long trapping time for practical applications.

Metamaterials with artificially engineered building blocks have attracted significant research interest during the past decade. These materials exhibit unusual electromagnetic properties such as negative refraction,[1] breaking down of the diffraction limit in imaging,[2–4] and invisible cloaking.[4–6] The macroscopic response of metamaterials can be flexibly tailored to achieve exotic media, such as left-handed materials (LHMs) simultaneously exhibiting negative permittivity and permeability,[7] ultrahigh-refractive-index materials,[8,9] zero-index materials, and hyperbolic metamaterials (HMMs) with strong anisotropy.[10–12] A high-refractive-index metamaterial can significantly reduce the size of an optical device,[13] and a zero-index material can help achieve directive radiation.[14] A LHM can be utilized to greatly reduce the group velocity of a pulse of light within a waveguide structure, by virtue of the opposite directions of energy flows in the waveguide core layer and the cladding layer.[15–19] When the waveguide structure is carefully tuned, the group velocity of a pulse of light can even approach zero. Nonetheless, the realization of these structures is limited because of the difficulties and expenses of fabrication at IR and visible light. HMM, which can support a similar phenomenon,[20] is a promising solution to this problem since it is relatively easy to fabricate. Some techniques have been developed to fabricate tapered HMM waveguides with an on-demand filling ratio.[21] Recently, a tapered metamaterial waveguide has been proposed to completely stop incident white light and trap it forever to form the so-called "trapped rainbow".[22] However, we have clearly shown that the incident light will eventually be reflected back owing to strong intermodal coupling.[23]

In this work, we would like to provide a comprehensive analysis of the light trapping time inside a HMM waveguide. First of all, the intermodal-coupling-induced reflection of a pulse is clearly illustrated, and the light trapping time is unambiguously defined. Then, the dependence of the light trapping time on the filling ratio and material dispersion is thoroughly investigated. A mode-matching technique is employed in our trapping time calculation. Finally, as the light trapping time is always finite in a single-tapered waveguide, the design methods of the HMM waveguides to prolong the light trapping time are discussed.

Figure 1(a) shows a schematic of a multilayer structure with alternative ultrathin metal–dielectric stacks. As the multilayer structure is subwavelength-scaled, it could be treated as a homogeneous effective medium, and the principal components of the permittivity tensor are then determined from the effective medium theory:

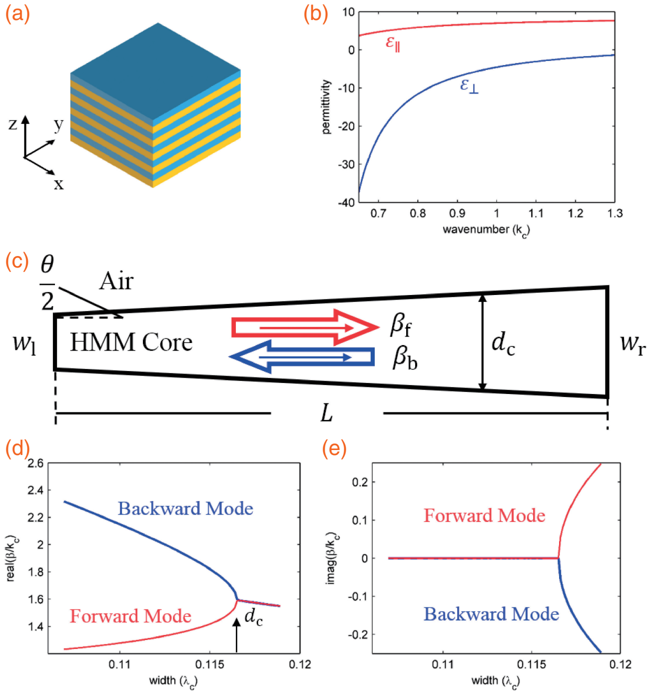

Fig. 1. (a) Structure of a multilayer HMM. The material is composed of alternating layers of metallic (yellow) and dielectric (blue) materials. (b) Variation of permittivity tensors of the HMM with wavenumber. $\varepsilon_z = \varepsilon_\perp < 0$, $\varepsilon_x = \varepsilon_\parallel > 0$. (c) Schematic of a HMM slow-light waveguide. The thick open arrows show the direction of the energy flow, while the thin arrows inside the thick open arrows indicate the direction of the wave vector. β_f, β_b, and θ stand for the propagation constants of the forward wave (indicated by the red arrows that point to the same direction) and the backward wave (indicated by the blue arrows that point to opposite directions), and the tapering angle, respectively. (d, e) Propagation constants of the forward (red curve) and backward (blue curve) modes (at the central wavelength of λ_c) as the width of the HMM core varies.

$$\begin{cases} \varepsilon_x = \varepsilon_\parallel = f_\mathrm{m}\varepsilon_\mathrm{m} + (1-f_\mathrm{m})\varepsilon_\mathrm{d} \\ \varepsilon_z = \varepsilon_\perp = \dfrac{\varepsilon_\mathrm{m}\varepsilon_\mathrm{d}}{f_\mathrm{m}\varepsilon_\mathrm{d} + (1-f_\mathrm{m})\varepsilon_\mathrm{m}} \end{cases}, \qquad (1)$$

where f_m is the volume filling ratio of the metallic material, and ε_d and ε_m are the permittivities of the dielectric and metallic materials, respectively. In our study, $\varepsilon_d = 16$, and the response of the metallic material, $\varepsilon_m(\omega)$, is determined using the Lorentz model:

$$\varepsilon_m = \varepsilon_\infty + \frac{\omega_p^2}{\omega_0^2 - \omega^2 - i\gamma\omega}, \tag{2}$$

where ω_0 and $\varepsilon_\infty = 1$ are the resonance frequency and the background dielectric constant, respectively. The material loss is neglected here for simplicity, while its impact on light trapping performance will be discussed at the end of this paper. The calculated effective medium permittivity tensors of a sample HMM with $f_m = 0.5$, $\omega_0 = 0.2\omega_c$, and $\omega_p = 1.59\omega_c$ are opposite in sign [shown in Fig. 1(b)]. Herein, ω_c is the central frequency of the incident light pulse. This leads to the hyperbolic properties of the isofrequency surface of the structure, which is given by[24]

$$\frac{k_x^2}{\varepsilon_\parallel} + \frac{k_z^2}{\varepsilon_\perp} = \left(\frac{\omega}{c}\right)^2, \tag{3}$$

where k_x and k_z are, respectively, the x and z components of the wave vector, ω is the wave frequency, and c is the speed of light.

The schematic of a typical HMM slow-light waveguide is shown in Fig. 1(c), which is composed of a HMM core and air cladding. The waveguide is linearly tapered from the left port with width w_l to the right port with width w_r within the length L. Owing to the hyperbolic property of the metamaterial, two modes with distinct properties coexist in the metamaterial waveguide: the forward mode, whose energy flow and wave vector are in the same direction, and the backward mode, whose energy flow and wave vector are in opposite directions. The relationships of the propagation constants of the forward and backward modes with the core width at the central wavelength λ_c are presented in Figs. 1(d) and 1(e). The propagation velocities of both modes become increasingly smaller as the core layer width gradually increases. It is noted that the forward and backward modes will degenerate at a critical thickness (denoted by d_c), where the light velocity becomes exactly zero. At first glance, a tapered slow-light waveguide seems capable of stopping the incident light and trapping it at the critical thickness forever. However, the incident light is actually reflected back owing to the intermodal coupling between the forward and backward modes at d_c.[23] Nonetheless, it may still be sufficient to trap light over a relatively long time for some applications. Therefore, the trapping time in such a metamaterial waveguide is comprehensively investigated in this work.

Figure 2 shows the behavior of an incident pulse of light inside such a tapered waveguide with $w_l = 0.107\lambda_c$, $w_r = 0.119\lambda_c$, and $L = 60\lambda_c$. The material parameters are of the same value as in the calculation shown in Fig. 1. The field is calculated by a mode-matching technique and frequency component superposition around the central wavelength λ_c.[25] In our calculation, the light pulse is located at the input port at $t = 0$. It will propagate towards the output port as time elapses. At the critical thickness, the strong intermodal coupling between the two guided modes will reverse the propagation direction of the pulse. Finally, the pulse will flow out from the input port at $t = \tau$. The time interval between 0 and τ is defined as the light trapping time for a certain metamaterial waveguide. A longer waveguide length corresponds to a longer trapping time, so the waveguide length L is fixed at $60\lambda_c$ when we talk about trapping time in our study.

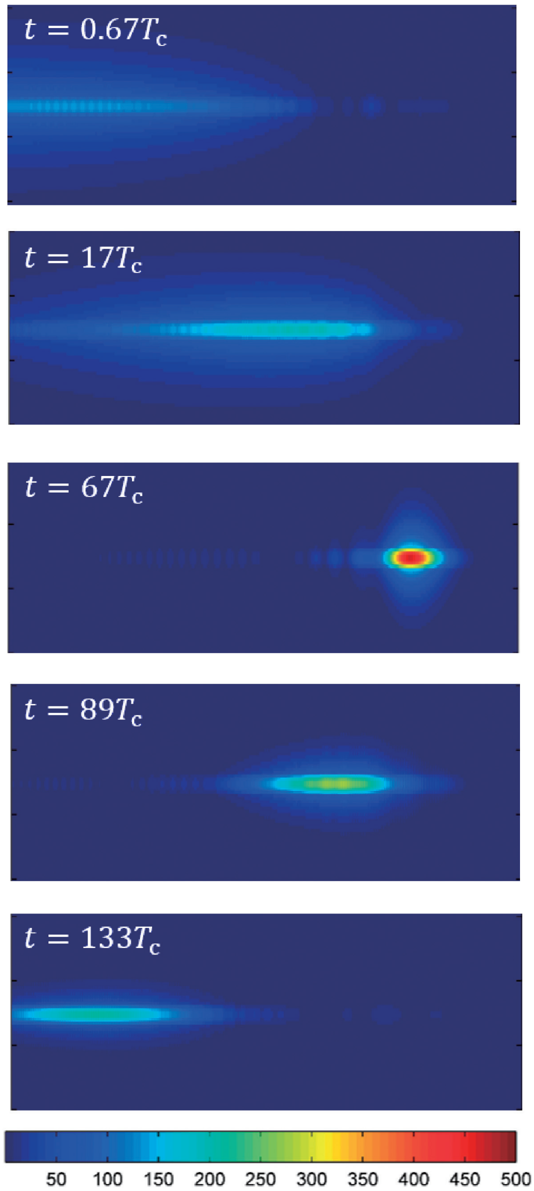

Fig. 2. Propagation and reflection of a guided wave packet in time domain in a tapered slow-light metamaterial waveguide. The field patterns of $|H_y|$ at different times after the pulse enters the tapered HMM slow-light waveguide are shown. The light trapping time is normalized by the period of the central wavelength $T_c = 2\pi/\omega_c$.

First, we study the optimization of trapping time by changing the volume filling ratio of the HMM slow-light waveguide. The filling ratio ranges from 30 to 70% in steps of 10%. Figure 3(a) shows the relationship between the critical thicknesses and the propagation constants of different filling ratios at the central wavelength. It is clear that for a fixed frequency, the critical thickness becomes larger as the filling ratio increases. To make a fair comparison, the structures of the waveguides are designed to ensure that the position with critical thickness is always located at 80% of the length L to the left port while the tapering angle is fixed at $\theta = 2 \times 10^{-4}$ rad. The specific parameters of the waveguides can be found in Table I. By performing the mode-matching calculation, the light trapping times are obtained. Figure 3(b) shows the evolution of the magnetic field intensity with time

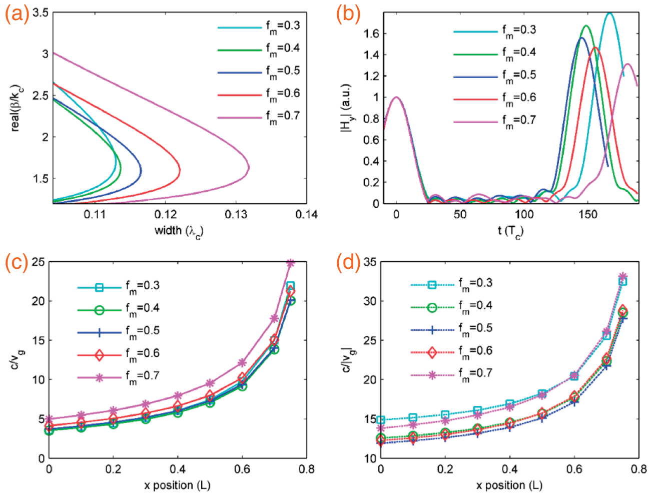

Fig. 3. Light trapping by HMM slow-light waveguides with different volume filling ratios. (a) Variation of critical thicknesses of waveguides with different filling ratios. (b) Magnetic field intensities at the incident port of the HMM waveguides as functions of time. (c, d) Values of the light slow-down factor $c/|v_g|$ of the (c) forward and (d) backward modes (at the central wavelength).

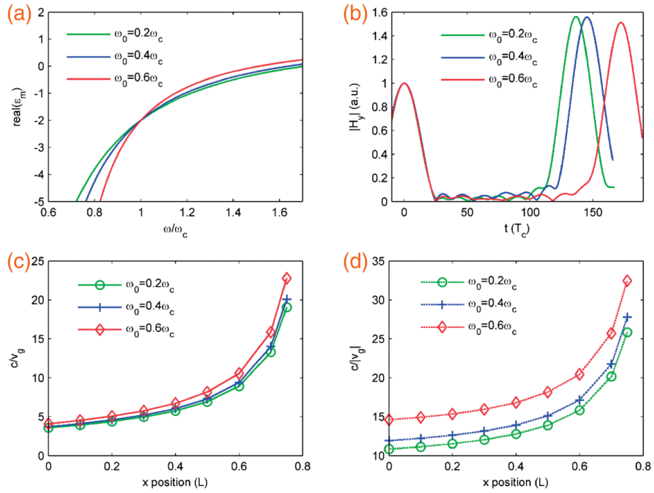

Fig. 4. Light trapping by HMM slow-light waveguides composed of metallic materials with different dispersions. (a) Permittivities of three different metallic materials as the frequency varies. (b) Magnetic field intensities at the incident port of the HMM waveguides as functions of time. (c, d) Values of $c/|v_g|$ of the (c) forward and (d) backward modes (at the central wavelength).

Table I. Parameters of the HMM waveguide with different filling ratios. The lengths of these waveguides are the same, and the position with critical thickness d_c at the central wavelength is at the same location, i.e., 80% of L to the left incident port.

f_m	$w_l(\lambda_c)$	$w_r(\lambda_c)$	$\tau(T_c)$
0.3	0.103	0.115	167
0.4	0.104	0.116	149
0.5	0.107	0.119	145
0.6	0.112	0.124	156
0.7	0.122	0.134	181

Table II. Parameters of the HMM waveguide composed of metallic materials with different dispersions. The metallic materials have the same $\varepsilon_m = -2$ at the central wavelength. The position with critical thickness d_c is located at 80% of L to the left incident port.

$\omega_0(\omega_c)$	$\omega_p(\omega_c)$	$\tau(T_c)$
0.2	1.70	136
0.4	1.59	145
0.6	1.39	183

at the left port for five different waveguides. The time interval between the two peaks is exactly the trapping time that we defined, and it is given in Table I. It is clear that the trapping time will first decrease as the filling ratio increases from 30 to 50%. After that, the trapping time becomes longer as the filling ratio increases beyond 50%. This phenomenon could be explained below by comparing the group velocities ($v_g \equiv d\omega/dk \mid \omega = \omega_c$) at different positions of the waveguides.

First, the situations with $f_m \leq 0.5$ are discussed. As shown in Figs. 3(c) and 3(d), the light slow-down factor $c/|v_g|$ of the forward mode decreases slightly as f_m increases while the signal propagates along the waveguide towards d_c. The $c/|v_g|$ of the backward mode also decreases as f_m increases. However, it is noted that the $c/|v_g|$ of the backward mode is larger than that of the forward mode, and $c/|v_g|$ decreases much faster for the backward mode than for the forward mode. The tendencies remain true from the incident port to the critical thickness, and both the forward and backward modes contribute to the light trapping time of the incident pulse. Therefore, a longer light trapping time is obtained for HMM with a smaller f_m.

For the filling ratio $f_m \geq 0.5$, the light trapping tendency is reversed. The $c/|v_g|$ of both the forward and backward modes will increase as f_m increases. Thus, a longer trapping time will be achieved in the HMM waveguide with a larger f_m. These conclusions are consistent with the light pulse calculation shown in Fig. 3(b) and Table I.

Here, it is also interesting to compare the light trapping performances when two slow-light waveguides have complementary volume filling ratios (e.g., 30 and 70%, and 40 and 60%). It is found that a larger volume filling ratio will lead to a longer trapping time. The $c/|v_g|$ values of the backward modes of the structures with larger filling ratios are slightly smaller than those of their complementary counterparts. Nonetheless, this factor of the forward modes of such structures is considerably larger, which enables an overall lower average travelling speed of the materials with larger filling ratios, and consequently leads to a longer trapping time.

Next, the effect of material dispersion on light trapping time is explored. Different metamaterials can have the same permittivity at a specific working frequency but different material dispersions $d\varepsilon/d\omega$. It is expected that the material dispersion will have a great impact on the group velocity of guided modes. Figure 4(a) plots the material dispersions for three different metallic materials that are used to construct the HMM waveguides. The permittivity of the material follows Eq. (2). The material parameters (see Table II) are carefully chosen so that all the metallic materials have the same $\varepsilon_m(\omega_c) = -2$ at the central frequency but different material dispersions.

A tapered HMM waveguide with 50% filling ratio is chosen for the trapping time comparison. The evolution of the magnetic field with time is plotted in Fig. 4(b), and the trapping times (see Table II) are derived by the same method as in our previous calculations. It is found that a higher resonance frequency will lead to a longer trapping time. Similar to the analysis shown in Fig. 3, the $c/|v_g|$ values at different locations of the waveguides are presented in Figs. 4(c) and 4(d) to interpret the light trapping results. It is evident that the metamaterial with a larger ω_0 will always result in a larger $c/|v_g|$, which holds true for both the forward and backward modes. This leads to a lower average light travelling speed and thus a prolonged trapping time.

On the basis of previous calculations, it can be concluded that although the light could not be trapped in a tapered HMM waveguide forever, the structure of the waveguide can be optimized to prolong the light trapping time. Fabricating materials with filling ratios away from 50% and using metallic materials with high resonance frequencies can significantly enhance the light trapping effects.

One thing that should be noted is that the material loss is neglected in our theoretical studies even though material loss is inevitable in a realistic metamaterial structure. The loss will lead to the decay of the trapped light energy, especially when the volume filling ratio is large. However, the trapping time of the light signal is negligibly affected, according to our calculations (not shown here). To further optimize the working conditions of the design, some approaches should be employed to reduce the effects of the loss, such as using low-loss novel materials[26] or the use of active gain materials.[27–29]

In summary, we studied the light trapping phenomenon in a tapered slow-light HMM waveguide. The light trapping time can be prolonged by optimizing structures with appropriate volume filling ratios and using metallic materials with large resonance frequencies. The reason for the light trapping time enhancement was interpreted by comparing the group velocities along the tapered slow-light waveguide. The results could shed light on the development of HMM waveguides for future applications, such as light storage and light enhancement.

Acknowledgments This work was partially supported by the National High Technology Research and Development Program (863 Program) of China (No. 2012AA030402), the National Natural Science Foundation of China (Nos. 91233208 and 61178062), the Program of Zhejiang Leading Team of Science and Technology Innovation, and Swedish VR grant (No. 621-2011-4620).

1) D. R. Smith, J. B. Pendry, and M. C. K. Wiltshire, Science **305**, 788 (2004).
2) J. B. Pendry, Phys. Rev. Lett. **85**, 3966 (2000).
3) N. Fang, H. Lee, C. Sun, and X. Zhang, Science **308**, 534 (2005).
4) J. B. Pendry, Prog. Electromagn. Res. **147**, 117 (2014).
5) J. B. Pendry, D. Schurig, and D. R. Smith, Science **312**, 1780 (2006).
6) D. Schurig, J. J. Mock, B. J. Justice, S. A. Cummer, J. B. Pendry, A. F. Starr, and D. R. Smith, Science **314**, 977 (2006).
7) D. R. Smith, W. J. Padilla, D. C. Vier, S. C. Nemat-Nasser, and S. Schultz, Phys. Rev. Lett. **84**, 4184 (2000).
8) J. T. Shen, P. B. Catrysse, and S. Fan, Phys. Rev. Lett. **94**, 197401 (2005).
9) Y. He, S. He, J. Gao, and X. Yang, J. Opt. Soc. Am. B **29**, 2559 (2012).
10) M. Silveirinha and N. Engheta, Phys. Rev. Lett. **97**, 157403 (2006).
11) A. Alù, M. G. Silveirinha, A. Salandrino, and N. Engheta, Phys. Rev. B **75**, 155410 (2007).
12) J. Elser, R. Wangberg, V. A. Podolskiy, and E. E. Narimanov, Appl. Phys. Lett. **89**, 261102 (2006).
13) M. Choi, S. H. Lee, Y. Kim, S. B. Kang, J. Shin, M. H. Kwak, K.-Y. Kang, Y.-H. Lee, N. Park, and B. Min, Nature **470**, 369 (2011).
14) S. Enoch, G. Tayeb, P. Sabouroux, N. Guérin, and P. A. Vincent, Phys. Rev. Lett. **89**, 213902 (2002).
15) A. Peacock and N. Broderick, Opt. Express **11**, 2502 (2003).
16) I. V. Shadrivov, A. A. Sukhorukov, and Y. S. Kivshar, Phys. Rev. E **67**, 057602 (2003).
17) J. He and S. He, IEEE Microwave Wireless Components Lett. **16**, 96 (2006).
18) W. T. Lu, Y. J. Huang, B. D. F. Casse, R. K. Banyal, and S. Sridhar, Appl. Phys. Lett. **96**, 211112 (2010).
19) M. S. Jang and H. Atwater, Phys. Rev. Lett. **107**, 207401 (2011).
20) W. T. Lu and S. Sridhar, Phys. Rev. A **82**, 013811 (2010).
21) P. R. West, N. Kinsey, M. Ferrera, A. V. Kildishev, V. M. Shalaev, and A. Boltasseva, Nano Lett. **15**, 498 (2015).
22) K. L. Tsakmakidis, A. D. Boardman, and O. Hess, Nature **450**, 397 (2007).
23) S. He, Y. He, and Y. Jin, Sci. Rep. **2**, 583 (2012).
24) A. Poddubny, I. Iorsh, P. Belov, and Y. Kivshar, Nat. Photonics **7**, 948 (2013).
25) Ş. E. Kocabaş, G. Veronis, D. A. B. Miller, and S. Fan, Phys. Rev. B **79**, 035120 (2009).
26) A. Boltasseva and H. A. Atwater, Science **331**, 290 (2011).
27) C. M. Soukoulis and M. Wegener, Science **330**, 1633 (2010).
28) S. Xiao, V. P. Drachev, A. V. Kildishev, X. Ni, U. K. Chettiar, H.-K. Yuan, and V. M. Shalaev, Nature **466**, 735 (2010).
29) R. S. Savelev, I. V. Shadrivov, P. A. Belov, N. N. Rosanov, S. V. Fedorov, A. A. Sukhorukov, and Y. S. Kivshar, Phys. Rev. B **87**, 115139 (2013).